

Additive-Free Fabrication of Spherical Hollow Palladium/Copper Alloyed Nanostructures for Fuel Cell Application

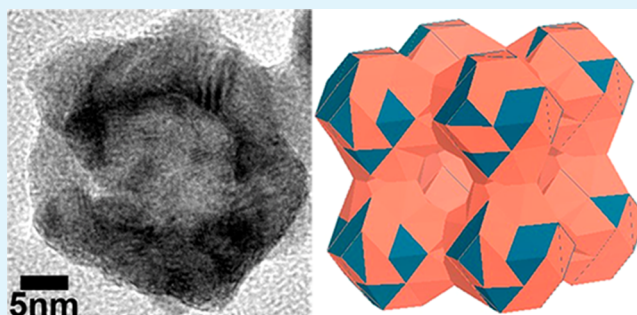
Chuangang Hu,^{†,§} Yuming Guo,^{†,§} Jinlong Wang,[‡] Lin Yang,^{*,†} Zongxian Yang,^{*,‡} Zhengyu Bai,[†] Jie Zhang,[†] Kui Wang,[†] and Kai Jiang[†]

[†]College of Chemistry and Chemical Engineering, Key Laboratory of Green Chemical Media and Reactions, Ministry of Education, and [‡]College of Physics & Information Engineering, Henan Normal University, Xinxiang, 453007, P.R. China

Supporting Information

ABSTRACT: Herein, through tuning the surface energy difference of the major crystal planes by alloying, hollow palladium/copper alloyed nanostructures are successfully prepared through a one-pot template-free strategy. Compared with the solid PdCu alloyed nanoparticles, the hollow PdCu alloyed nanostructures exhibit the increased accessible electrochemical active surface area and the enhanced electrocatalytic activity for formic acid oxidation. It is concluded that the as-prepared hollow PdCu alloyed nanostructures would be a potential candidate as an anode electrocatalyst in direct formic acid fuel cell. More importantly, the strategy developed in this study might be expanded to fabricate other metal alloyed hollow nanostructures.

KEYWORDS: palladium/copper alloy, hollow nanostructure, surface energy difference, electrocatalytic activity, direct formic acid fuel cell, formic acid oxidation



Nowadays, noble metals are extensively utilized as catalysts in various fields, including organic chemistry and fuel cells.^{1,2} Nevertheless, the rare reserve and rapidly rising price of the noble metals severely limited the applications of the noble metal catalysts. Therefore, tremendous efforts have been made to solve these issues, in which a general strategy is to form the alloyed nanoparticles of noble and non-noble metals. Previous studies demonstrated that some alloyed catalysts exhibited significant enhancement of the catalytic activity and selectivity over the pure noble metals catalysts, and thereby reduce the costs of the catalysts.^{3–7} On the other hand, because of the lower densities and higher specific surface areas, hollow nanostructures of noble metals exhibited significantly improved catalytic performance and utilization efficiency, and thereby reduced the costs of the catalysts efficiently.^{8–10} Therefore, the construction of hollow metal nanostructures is considered as an important strategy and attracts tremendous attention. Recently, the preparation of the single or bimetallic noble metal hollow structures using active metals as sacrificial templates was reported.^{11,12} However, the rigorous reaction conditions and poor reproducibility seriously limit the applications. Heretofore, the facile one-pot additive-free synthesis of hollow bimetallic nanostructures assembled by noble and non-noble alloyed nanoparticles is seldom reported and still remained a great challenge.

In our previous report, using glutamate as additive, hollow alloyed nanocubes were prepared through the adjustment of the surface energy difference (γ_{diff}) of the major crystal planes

by alloying.¹⁰ Herein, spherical hollow palladium/copper alloyed nanostructures supported on multiwalled carbon nanotubes (PdCu/MWCNTs) are prepared by alloying through a facile one-pot method. It should be noted that this method is additive-free and suitable for one-pot synthesis of hollow nanostructures assembled by alloyed nanoparticles of noble and non-noble metals. Moreover, through the introduction of right amount of Cu, the lattice parameter of the alloy was finely tuned to relieve the undesirable hydrogen absorption to improve the free accessible surface active sites by small molecules for electrooxidation. This could enhance the electrocatalytic performance significantly, which lowered the loading amount of Pd and the cost of the catalyst obviously.

For the facile preparation of the PdCu/MWCNTs, palladium^{II} salt and copper^{II} salt (1:1 atomic ratio), and MWCNTs were simultaneously dispersed into ethylene glycol (EG) in a stainless-steel autoclave, and the pH was adjusted to 12. Then it was sealed and heated at 160 °C for 6 h to prepare the PdCu/MWCNTs.

The transmission electron microscopy (TEM) observation indicates the successful preparation of the PdCu/MWCNTs. From Figure 1a, the hollow nanospheres with the average diameter of ca. 40 nm are composed of an empty core with a uniform shell with the average thickness of 4 nm. In addition,

Received: July 17, 2012

Accepted: August 31, 2012

Published: August 31, 2012

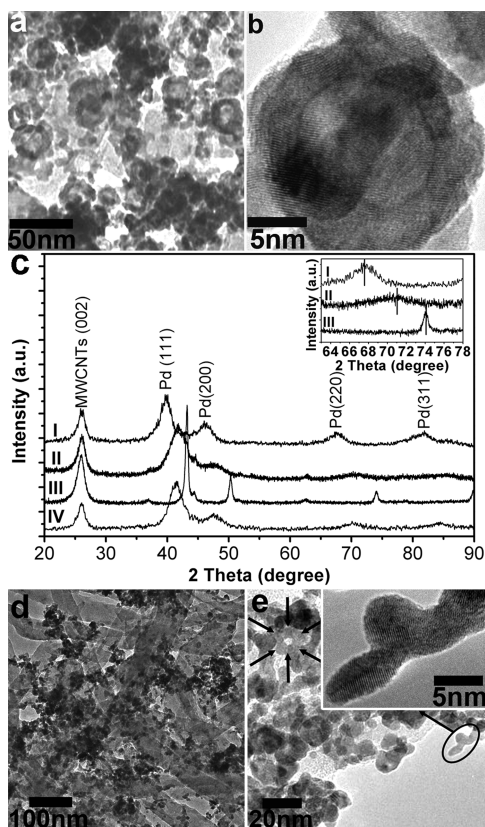


Figure 1. (a) TEM and (b) HRTEM image of the PdCu/MWCNTs. (c) XRD pattern of the PdCu/MWCNTs. Curve I, Pd/MWCNTs; curve II, PdCu/MWCNTs; curve III, Cu/MWCNTs, curve IV, PdCu alloyed nanoparticles. TEM images of samples obtained at (d) 1 h and (e) 3 h; inset, HRTEM image.

the high resolution TEM (HRTEM) further indicates the formation of the hollow nanospheres and the hollow nanospheres are coalesced by small PdCu alloyed nanoparticles (Figure 1b). The composition of the PdCu/MWCNTs was determined as 1:1 atomic ratio of Pd and Cu through energy-dispersive X-ray spectroscopy (EDS) measurement (see Figure S1 in the Supporting Information), in accordance with the theoretical stoichiometric proportion.

Powder X-ray diffraction (XRD) results indicate the successful formation of the PdCu alloys. Figure 1c shows the XRD patterns of Cu supported on MWCNTs (Pd/MWCNTs, curve I), PdCu/MWCNTs (curve II), and Pd supported on MWCNTs (Cu/MWCNTs, curve III), respectively. For the Pd/MWCNTs, the first peak at 26.06° is attributed to the (002) plane of the MWCNTs,⁷ the other four peaks at 39.75° , 46.32° , 67.40° , and 81.89° are assigned to the (111), (200), (220), and (311) planes of the face-centered-cubic (fcc) Pd, respectively. Compared with the Pd/MWCNTs, the diffraction peaks of the PdCu/MWCNTs slightly shift to the higher 2θ values. Furthermore, the peak at 74.25° in curve III characteristic to Cu (220) plane disappears in curve II and the lattice parameter of the PdCu/MWCNTs (0.3770 nm) lies between those of Pd (0.3885 nm) and Cu (0.3605 nm). These results demonstrate the successful formation of the PdCu alloys.^{10,13} In addition, the (200) diffraction peak of Pd in curve I almost disappears in curve II after the formation of the alloys. This might be attributed to the oriented attachment through

(200) plane during the formation of the hollow alloyed nanostructures.

To determine the formation mechanism of the hollow nanospheres, we monitored the samples at different intervals during the formation process. The XRD and EDS results obviously indicate the formation of the PdCu alloys for 1 h (Figure 1c, Figure S2, Supporting Information). From the TEM image shown in Figure 1d, only PdCu alloyed nanoparticles are formed after 1 h. After reacted for 3 h, the tendency of the formation of hollow structures is very obvious (Figure 1e). The inset of Figure 1e clearly reveals the oriented attachment of PdCu alloyed nanoparticles. After reacted for 6 h, the hollow nanospheres are formed and the internal void space in nanospheres becomes more distinct. Therefore, it can be proposed that the initial formation of the PdCu alloyed nanoparticles and the subsequent oriented attachment play the important roles in the formation of the hollow PdCu alloyed nanospheres.

To better understand the formation mechanism of the hollow nanospheres by coalescence of the alloyed nanoparticles, we carried out the theoretical calculations using density functional theory (DFT) by introducing the surface energy (γ), which is the surface excess free energy per unit area of a certain crystal plane and plays the important roles in crystal growth.¹⁴ From the results, the surface energies of the Cu (111) and (100) and Pd (111) and (100) are 1.28, 1.33, 1.31, and 1.48 J m^{-2} , respectively, in coincidence with the previous reports.^{10,15} The $\gamma_{(111)}$ of the PdCu alloys is calculated as 1.29 J m^{-2} , lying in between the values of Cu and Pd. While the calculated $\gamma_{(100)}$ of the PdCu alloys (1.59 J m^{-2}) is much higher than those of the pure counterparts (Figure 2a). Therefore the

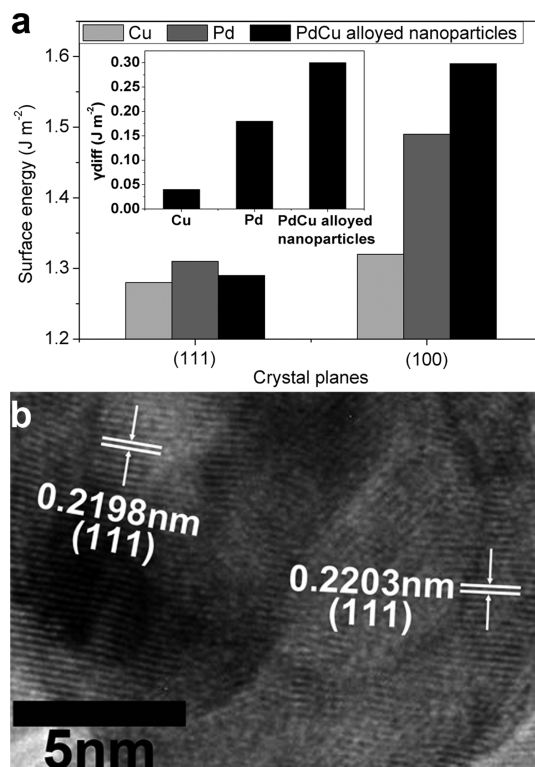


Figure 2. (a) Surface energies of the (111) and (100) planes of the Cu, Pd, and PdCu alloyed nanoparticles. Inset: the γ_{diff} between (100) and (111) planes of the Cu, Pd, and PdCu alloyed nanoparticles. (b) HRTEM image of the PdCu/MWCNTs.

γ_{diff} between the (111) and (100) planes of the PdCu alloyed nanoparticles is much higher than those of the pure counterparts. Consequently, after the formation of the alloyed nanoparticles, the metastable alloyed nanoparticles would self-assemble and coalesce through the oriented attachment of the high energy (100) plane, which will result in the reduction of the total energy of the system. This might be the driving force for the formation of the hollow PdCu nanospheres. Indeed, the hollow PdCu nanospheres obtained in the typical experiment mainly present the (111) plane (Figure 2b). In addition, compared with the XRD pattern of the PdCu alloyed nanoparticles (curve IV, Figure 1c), the diffraction peak of the (200) plane of the PdCu alloys almost disappears after the formation of the hollow alloyed nanospheres (curve II, Figure 1c). This further confirms the oriented attachment of the (100) plane during the formation of the hollow alloyed nanospheres. Furthermore, through the oriented attachment of the (100) planes of the model PdCu alloyed nanoparticles, a hollow model similar to the experimental result can be constructed theoretically (see Figures S3 and S4 in the Supporting Information). This confirms the reasonability of the above-described theoretical explanation.

The application of the as-prepared PdCu/MWCNTs as the electrocatalyst of the direct formic acid fuel cell (DFAFC) was evaluated. From the carbon monoxide (CO) stripping voltammetry studies (Figure 3), the electrochemical active

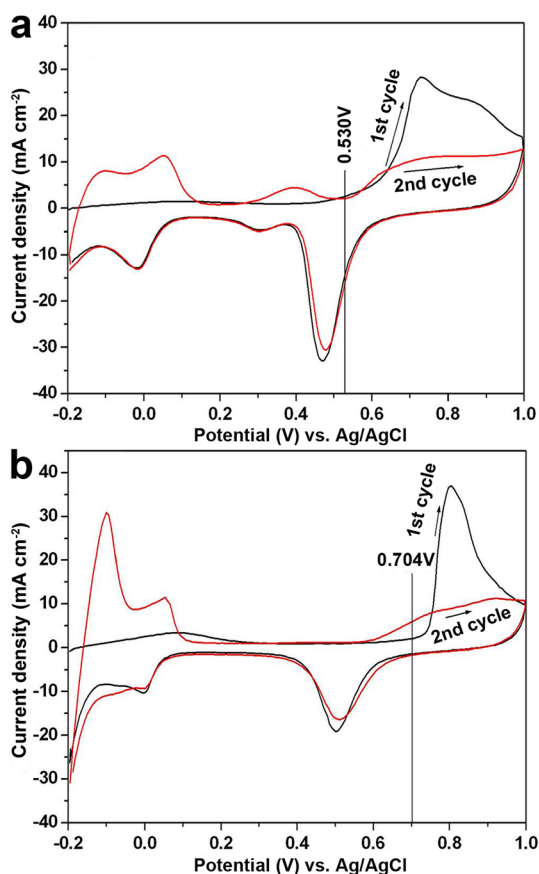


Figure 3. CO-stripping voltammograms of (a) the PdCu/MWCNTs and (b) the Pd/MWCNTs.

surface area (EAS) of the PdCu/MWCNTs is much larger than that of the Pd/MWCNTs. Furthermore, the onset potential of the CO-stripping on PdCu/MWCNTs shifts toward the

negative direction compared with the Pd/MWCNTs. This reveals that the EAS of the PdCu/MWCNTs is significantly higher than that of the Pd/MWCNTs, which may be attributed to two different reasons. First, compared with the PdCu alloyed nanoparticles, the internal void space of the hollow alloyed nanosphere can be considered as the additional internal surface.¹⁶ This can enhance the EAS accessible by small molecules (e.g., formic acid,) significantly, resulting in the improved utilization efficiency and thereby the higher electrocatalytic activity. Second, electronic effect between Pd and Cu might be another reason. Pd in the catalyst can gain the *d*-electrons from Cu of the alloys, which can relieve the adsorption strengths for CO, the important reaction intermediates in formic acid oxidation.¹⁷

Electrochemical measurements indicate that the PdCu/MWCNTs exhibits much better electrocatalytic activity for formic acid electrooxidation than the Pd/MWCNTs. From the results shown in Figure 4, the two main oxidation peaks of the

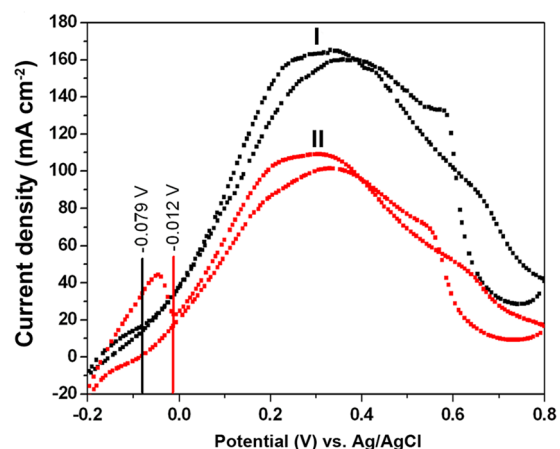


Figure 4. Cyclic voltammograms of the (I) PdCu/MWCNTs catalyst, (II) Pd/MWCNTs catalyst in 0.5 M H₂SO₄ + 0.5 M CH₃OH aqueous solution.

catalysts locate at ca. 0.30 V in both the positive and negative directions. The corresponding peak current density of the PdCu/MWCNTs in positive scan mode is 166.7 mA/cm², much higher than that of the Pd/MWCNTs (105.9 mA/cm²). Furthermore, the onset potential of formic acid electrooxidation locates near -0.079 V, much more negative than -0.012 V of the Pd/MWCNTs. The higher oxidation current and the lower onset potential demonstrate the much better electrooxidation activity of the PdCu/MWCNTs.¹⁸

From the chronoamperometry analysis results shown in Figure S5 (Supporting Information), the PdCu/MWCNTs exhibits the much higher anodic current and the slower current decay than that of the Pd/MWCNTs after 5000 s, indicating the better catalytic activity and the higher stability for formic acid electrooxidation. This further demonstrates that the formation of the hollow nanostructures can significantly enhance the catalytic activity and stability of the catalyst.

In summary, PdCu/MWCNTs can be prepared successfully by alloying through a facile one-pot additive-free method. The as-prepared PdCu/MWCNTs exhibit the enhanced accessible EAS and therefore the enhanced electrocatalytic activity for formic acid oxidation. Therefore, the PdCu/MWCNTs would be a potential candidate as an anode electrocatalyst in DFAFC. More importantly, the strategy presented in this work might be

expanded to fabricate other metal alloyed hollow nanostructures. For example, through this strategy, the preliminary results from the ongoing studies on the preparation of the PtCu and RhCu alloyed hollow nanostructures show the positive perspectives.

■ ASSOCIATED CONTENT

🔍 Supporting Information

Experimental details, EDS of PdCu/MWCNTs and PdCu nanoparticles, construction of the model hollow PdCu nanostructure, and chronoamperometric curves of the samples. This material is available free of charge via the Internet at <http://pubs.acs.org/>.

■ AUTHOR INFORMATION

Corresponding Author

*E-mail: yanglin1819@163.com (L.Y.); zongxian.yang@163.com (Z.X.Y.).

Author Contributions

§These authors contributed equally to this work and should be considered cofirst authors.

Notes

The authors declare no competing financial interest.

■ ACKNOWLEDGMENTS

This work was financially supported by the National Science Foundation of China (21171051, 21271066) and the Program for Changjiang Scholars and Innovative Research Team in University (IRT1061) and the Innovation Fund for Outstanding Scholar of Henan Province (114200510004) and Henan Key Proposed Program for Basic and Frontier Research (112102210005, 112300410095), and the Foundation for Key Young Teachers of Henan Province (2012GGJS-065) and Henan Normal University.

■ REFERENCES

- (1) Bell, A. T. *Science* **2003**, *299*, 1688–91.
- (2) Wu, X. F.; Anbarasan, P.; Neumann, H.; Beller, M. *Angew. Chem., Int. Ed.* **2010**, *49*, 9047–50.
- (3) Erlebacher, J.; Aziz, M. J.; Karma, A.; Dimitrov, N.; Sieradzki, K. *Nature* **2001**, *410*, 450–453.
- (4) Stamenkovic, V. R.; Mun, B. S.; Arenz, M.; Mayrhofer, K. J. J.; Lucas, C. A.; Wang, G.; Ross, P. N.; Markovic, N. M. *Nat. Mater.* **2007**, *6*, 241–247.
- (5) Xu, D.; Liu, Z.; Yang, H.; Liu, Q.; Zhang, J.; Fang, J.; Zou, S.; Sun, K. *Angew. Chem., Int. Ed.* **2009**, *48*, 4217–4221.
- (6) Wu, J.; Zhang, J.; Peng, Z.; Yang, S.; Wagner, F. T.; Yang, H. J. *Am. Chem. Soc.* **2010**, *132*, 4984–4985.
- (7) Guo, Y.; Hu, C.; Yang, L.; Bai, Z.; Wang, K.; Chao, S. *Electrochem. Commun.* **2011**, *13*, 886–889.
- (8) Hyuk, Im, S.; Jeong, U.; Xia, Y. *Nat. Mater.* **2005**, *4*, 671–675.
- (9) Vasquez, Y.; Sra, A. K.; Schaak, R. E. *J. Am. Chem. Soc.* **2005**, *127*, 12504–12505.
- (10) Yang, L.; Hu, C.; Wang, J.; Yang, Z.; Guo, Y.; Bai, Z.; Wang, K. *Chem. Commun.* **2011**, *47*, 8581–8583.
- (11) Liang, H.-P.; Zhang, H.-M.; Hu, J.-S.; Guo, Y.-G.; Wan, L.-J.; Bai, C.-L. *Angew. Chem., Int. Ed.* **2004**, *43*, 1540–1543.
- (12) Liu, B.; Li, H. Y.; Die, L.; Zhang, X. H.; Fan, Z.; Chen, J. H. *J. Power Sources* **2009**, *186*, 62–66.
- (13) Du, C.; Chen, M.; Wang, W.; Yin, G.; Shi, P. *Electrochem. Commun.* **2010**, *12*, 843–846.
- (14) Tyson, W. R.; Miller, W. A. *Surf. Sci.* **1977**, *62*, 267–276.
- (15) Singh-Miller, N. E.; Marzari, N. *Phys. Rev. B* **2009**, *80*, 235407.
- (16) Huang, X.; Zhang, H.; Guo, C.; Zhou, Z.; Zheng, N. *Angew. Chem., Int. Ed.* **2009**, *48*, 4808–4812.
- (17) Zhou, W.; Lee, J. Y. *Electrochem. Commun.* **2007**, *9*, 1725–1729.
- (18) Wang, X.-M.; Xia, Y.-Y. *Electrochim. Acta* **2009**, *54*, 7525–7530.